# Insights on hazardous metal bioaccessibility, and groundwater impacted by Zn residues from a legacy mine and risk evaluation of adjacent soils.

Walubita Mufalo [a]*, Takahiko Arima [a], Toshifumi Igarashi [a], Mayumi Ito [a], Tsutomu Sato [a], Shingo Tomiyama [a], Imasiku Nyambe [b], Carlito Baltazar Tabelin [c], Hokuto Nakata [d], Shouta Nakayama [d, e] and Mayumi Ishizuka [d]

[a] Division of Sustainable Resources Engineering, Faculty of Engineering, Hokkaido University, Sapporo 060-8628, Japan

[b] IWRM Centre/Geology Department, School of Mines, The University of Zambia, Lusaka 32379, Zambia

[c] Department of Materials and Resources Engineering Technology, Mindanao State University—Iligan Institute of Technology, Iligan City 9200, Philippines

[d] Faculty of Veterinary Medicine, Hokkaido University, Kita 18, Nishi 9, Kita-Ku, Sapporo 060-0818, Japan

[e] Biomedical Sciences Department, School of Veterinary Medicine, The University of Zambia, Lusaka P.O. Box 32379, Zambia

*Corresponding email: wmufalo@gmail.com

**Abstract**

This study explored the legacy impact of Zinc plant residues (ZPRs) in Kabwe, Zambia, on the environment and human health, particularly in light of the town's reputation for Pb pollution. ZPRs solid samples and groundwater within and around ZPRs zone were collected from the legacy mine, along with soils within a 10 km radius from the mine site. Bioaccessible fractions of Pb and Zn were elucidated by Japanese leaching test (JLT) and Simple Bioaccessibility Extraction Test (SBET). Cationic speciation of Pb and Zn from inhalable and ingestible ZPRs particles was investigated via sequential extraction. Groundwater in the ZPRs area showed higher Zn levels (1,490 mg/L) than Pb (1.7 mg/L). Elevated Zn concentration were facilitated by the presence of soluble Zn sulfates while Pb was constrained due to its precipitation as anglesite. Groundwater sampled outside the ZPRs area was within the Zambia regulatory limits (<0.5 mg/L for Pb and <1 mg/L for Zn). Inhalation exposure to <30 μm dust particles from ZPRs and soils near the mine indicated negligible risk, with <3% of bioaccessible Pb in artificial lysosomal fluid. Meanwhile, oral intake of ZPRs particles <250 μm revealed elevated bioaccessible fractions (36% for Pb and 70% for Zn). ZPRs cationic speciation of ingestible particles <30 μm, 30-75 μm, 75-150 μm and 150-250 μm indicated that the bioaccessible Pb predominantly emanated from labile Pb fractions under gastric conditions with pH<1. This was due to the dissolution of Pb associated with the exchangeable phase, carbonates, and iron/manganese oxides, however, only exchangeable/carbonate Pb was bioaccessible at pH<2. Hazard quotients indicated increased risks of Pb intoxication through the ingestion of ZPRs and soils near the legacy mine, with higher risks observed in children, emphasizing the need to remediate legacy mine wastes to reduce health risks and protect groundwater through monitoring in mining-affected regions.

**Keywords:** Zinc residues; bioaccessible fractions; groundwater; lead; zinc; Zambia

**Graphical Abstract**

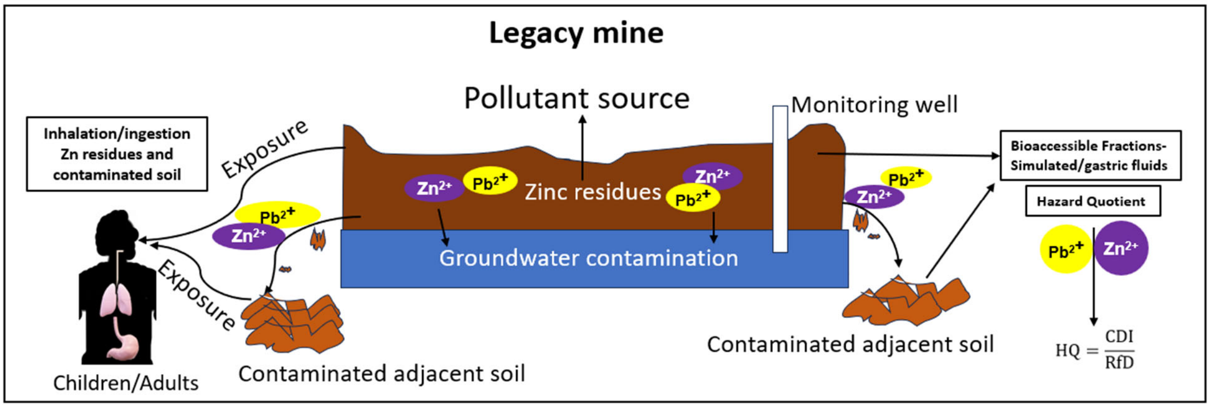

## 1. Introduction

Improper environmental practices during or after mining operations frequently result in significant environmental degradation upon the cessation of mining activities. Adverse effects of mining operations are largely attributed to the anthropogenic influences of the by-products generated during the mining process. The by-products produced from mining operations, such as tailings (Khoeurn et al., 2019), overburdened rocks (Singh and Narzary, 2021), and slag heaps (Ettler et al., 2020), constitute a substantial volume and frequently contain hazardous elements (HEs). The consequences following exposure to HEs have significant repercussions on both human health and the environment (Abraham et al., 2018; Reyes et al., 2021). Kabwe, a town in Zambia, serves as a typical example of the detrimental effects of mining activities. The town was once an industry hub for extracting Pb and Zn, with mining and processing operations carried out for nearly a century until the ore reserves were depleted in 1994 (Kamona and Fredrick, 2007). Numerous tons of mine wastes containing HEs, were left unattended, with the Zinc plant residues (ZPRs) occupying an extensive area over the legacy mine site (Nakamura et al., 2022; Nakata et al., 2022). The ZPRs have high contents of Pb and Zn, accounting for 10.9 % for Pb and 8.1 % for Zn (Tangviroon et al., 2020), which has potential to harm groundwater resources and soils.

Groundwater contamination (Tomiyama et al., 2019; Tomiyama and Igarashi, 2022) often arises from sulfide oxidation of mine wastes by acid mine drainage (AMD). For example, groundwater and surface water contamination in Sardinia, Italy was linked to sulfide oxidation of tailings stored in mine tunnels (Concas et al., 2006). Historical pollution of the Garonne-Gironde fluvial-estuarine system was partially attributed to Cd and Zn inputs from groundwater through the Riou Mort watershed (Coynel et al., 2007). Detrimental attributes are often reduced with proper disposal/monitoring system of abandoned mine (Nishimoto et al., 2021). None of these approaches were employed after the closure of the Kabwe mine; thus, contamination of groundwater from the ZPRs and dispersion of aerosols to the surrounding environment (Mufalo et al., 2023; Nakamura et al., 2021) are inevitable. Baieta et al. (2021) highlighted that the soil profiles around the Kabwe smelter had high concentrations of HEs in the top layers of soil and HEs were higher in soils closer to the smelter (up to 16,000 mg/kg Pb; 14,000 mg/kg Zn) compared to remote soils (up to 194 mg/kg Pb; 438 mg/kg Zn). Kříbek et al. (2019) and Tembo et al. (2006) have also conducted similar studies, including HEs in animals (Nakayama et al., 2011; Toyomaki et al., 2020) and blood Pb levels (BLLs) of the residents (Nakata et al., 2021; Yabe et al., 2020) neglecting the potential consequences of groundwater contamination by the ZPRs and bioaccessible Pb fractions emanating from inhalable and ingestible particles of the ZPRs.

Following accidental/intentional ingestion or inhalation of mine wastes/contaminated soil, only a fraction of the ingested HEs becomes solubilized/bioaccessible in gastric or lung fluids (Expósito et al., 2021; Guney et al., 2017; Pelfrêne et al., 2017, 2020; Soltani et al., 2021) and can be considered bioavailable (Meng et al., 2018). Semi-quantitative methods, such as batch leaching and sequential extraction that simulate natural environmental processes (Charlatchka and Cambier, 2000; Sungur et al., 2014) provide insights on release of HEs bound phases (Tabelin et al., 2018, 2020) and their solubility (Wiseman and Zereini, 2014). Bioaccessibility of HEs through inhalation or ingestion can be estimated by examining their solubility in simulated and gastric fluids that replicate conditions within the human body (Arenas-Lago et al., 2018; Behrooz et al., 2021; Li et al., 2021; Pelfrêne et al., 2020; Weggeberg et al., 2019), i.e., a fraction of the amount of the contaminant that is potentially available for absorption in human organs. Bioaccessibility of HEs has been studied by Boisa et al. (2014), Caboche et al. (2011), Guney et al. (2017), Kastury et al. (2017), Khan et al. (2022) and Khelifi et al. (2021). Although a standardized method for evaluating the bioaccessibility of HEs using simulated fluids is currently lacking (Caboche et al., 2011; Li et al., 2021), a variety of extraction fluids can be employed including artificial lysosomal fluid (ALF), Gamble solution (GS) and phosphate-buffered saline (PBS), to mimic conditions in human compartments. For example, ALF emulates the acidic fluid (pH 4.5) when macrophages interact with particles in the alveoli, while GS imitates interstitial lung fluid as described in the study by Pelfrêne et al. (2017). Phosphate-buffered saline mimics the ionic strength of solutions in the body (Caboche et al., 2011), whereas gastric fluids such as 0.4 M glycine, and 1 M hydrochloric acid are often used to imitate the fasting human gastric compartment in extreme pH conditions (Ether et al., 2019; Marove et al., 2022; Pelfrêne et al., 2020. Employing simulated/gastric fluids in convectional bioaccessibility tests does not ascertain HEs bound phases contributing to the bioaccessible fractions or whether these fractions entail potential hazard risks. Therefore, we integrated simulated and gastric fluids to examine bioaccessible fractions of distinct particle sizes of ZPRs from Kabwe legacy mine, the chemical forms of Pb/Zn; the major HEs in ZPRs and their partitioning discrepancies among various particle sizes to elucidate the potential hazard risks of Pb exposure emanating from ZPRs.

Seeking to bridge the existing knowledge gap on the potential health risks of ZPRs, in addition to evaluating their effects on groundwater and the related risks posed by soils in the vicinity of the Kabwe legacy mine, this study established four main objectives: (1) to evaluate the impact of the ZPRs on the groundwater within and around the ZPRs through monitoring wells installed at the historical mine; (2) to investigate the bioaccessible fractions of inhalable dust and ingestible particles originating from the ZPRs and adjacent soils via simulated and gastric fluids; (3) to elucidate elemental bound phases of distinct ingestible ZPRs particles responsible for bioaccessible Pb and Zn; and (4) to ascertain the human health risks posed by exposure to Pb and Zn from the legacy mine site.

## 2. Materials and Methods

### *2.1. Sample collection and preparation*

The Legacy mine in Kabwe, Zambia exhibits lithological formations characterized by Pb-Zn carbonate-hosted deposits (Kamona and Fredrick, 2007). Figure 1 shows the location of Kabwe and the sampling area for the ZPRs, groundwater monitoring wells KA-01, KA-02, KA-03 and soil samples S1 to S8. Groundwater samples were collected from monitoring well KA-01 located within the ZPRs and from KA-02 and KA-03 located outside the ZPRs. KA-01 was installed at a slightly higher elevation with respect to KA-02 and KA-03. Depth and elevation of each monitoring well is shown in Fig. S1. Groundwater samples were filtered using non-pyrogenic 0.45μm Millex®-HA (Merck, Millipore Ltd., Carrigtwohill, Ireland) syringe-driven sterile membrane filters and stored in air-tight containers prior to chemical analysis. Alkalinity was determined by titrating a known volume of groundwater with 0.01 M reagent-grade sulfuric acid ($H_2SO_4$) until reaching a pH of 4.8. The pH (HM-30P, DKK-TOA, Tokyo, Japan), oxidation reduction potential (ORP) (RM 30P, DKK-TOA Corporation, Tokyo, Japan) and electrical conductivity (EC) (CM-31P, CM-31P-W, DKK-TOA Corporation, Tokyo, Japan) were measured on site. The anion ($Cl^-$and $SO_4^{2-}$) concentrations were determined by ion chromatography (Dionex Integrion RFIC System, Thermo Fisher Scientific K.K., Tokyo, Japan). Major cations (Na, K, Ca, and Mg), Fe, Pb and Zn concentrations were determined using inductively coupled plasma atomic emission spectrometer (ICP-AES) (ICPE-9000, Shimadzu Corporation, Kyoto, Japan).

Agglomerated ZPRs particles were collected randomly from the mine site and subjected to light crushing with an agate mortar and pestle. The solid samples were then air-dried and subjected to sieving through a set of aperture screens, including <30 μm, 30-75 μm, 75-150 μm and 150-250 μm stainless sieves. Soil samples S1 to S8 were collected at depth of 5 cm, air dried and sieved using screens of <30 μm and <250 μm. Laser diffraction (Microtrac®

MT3300SX, Nikkiso Co. Ltd., Osaka) was used to assess the particle size variability in aerosols from both the ZPRs and soil samples for <30 μm particles. Typically, particles <62.5 μm are prone to wind dispersion, depending on the particle classification (Kok et al., 2012). In this study, inhalable dust was evaluated from aerosols <30 μm. Figure S2 illustrates the comparison of the particle size distribution for the <30 μm particles. About 50% of particles exhibited an effective diameter of <20 μm; easily deposited in the respiratory tract following accidental inhalation of contaminated soil/residues (Guney et al., 2017). The ZPRs exhibited the highest volume of <10 μm particles; accessible to the tracheobronchial region of the human lungs (Guney et al, 2017; Li et al., 2021).

***2.2. Sample characterization and digestion procedure***

Mineralogy and chemical composition of samples (<50 μm diameter) were measured using an X-ray diffractometer (XRD) (MultiFlex, Rigaku Corporation, Tokyo, Japan) and an X-ray fluorescence spectrometer (XRF) (SpectroXepos, Rigaku Corporation, Tokyo, Japan), respectively. Identification of all XRD patterns was conducted utilizing Match!® software (Crystal Impact, version 3.3.8, Bonn, Germany). The XRF results were expressed as contents of $Fe_2O_3$, $SiO_2$, $SO_3$, $TiO_2$, CaO, $Al_2O_3$, MgO, $Na_2O$, $K_2O$, MnO and trace elements. Total content of Pb and Zn for the <30 μm, ingestible particles <250 μm (US EPA, 2000) and bulk samples was measured via digestion using aqua regia (AR) (HC*l*/$HNO_3$, 3:1 solution).

***2.3. In-vitro solubility and bioaccessibility tests***

The solubility of Pb and Zn in the ZPRs/soil samples were investigated through solubility leaching tests in simulated fluids, such as ALF, GS, and PBS, and gastric fluids (1 M HC*l* and 0.4 M glycine) using Japanese leaching test JLT-46 Environment Agency Notification No.46, an environmental standard for wastes and soil, JLT-18 MOEJ Notification No. 19, an acid extraction test for oral intake, and Simple Bioaccessibility Extraction Test (SBET). Procedures for oral ingestion of ZPRs and soil included the use of 3g (<250 μm) of solid samples in 100 mL of 1 M HC*l*; followed by reciprocal shaking at 200 rpm for 2 hr, this test was performed to represent extreme gastric conditions of pH<1. SBET tests were conducted via adjusting 0.4 M glycine to pH 1.5 ± 0.05 using reagent grade HC*l*; S(<250 μm)/L ratio of 1/100 at 100 rpm for 1 hr, set at a temperature of 37°C using a bioshaker with temperature accuracy of ±0.1~±0.5°C (BR-21FH, Taitec Corporation, Koshigaya City, Saitama, Japan). This test was performed to represent gastric conditions of pH<2. The leachates were filtered through non-pyrogenic 0.45µm Millex®-HA and stored in air-tight containers.

Concentrations of Pb and Zn in the leachates were analyzed using inductively coupled plasma atomic emission spectroscopy (ICP-AES). Preparations of simulated fluids were adopted from Pelfrêne et al. (2017). The fluid compositions are listed in Table S1. Each batch of simulated fluids was formulated using reagent grade chemicals (Wako Pure Chemical Industries Ltd., Osaka, Japan), subsequently, the batches were stored in airtight 500 mL containers prior to solubility leaching experiments with the ZPRs and soil samples. To assess the solubility of Pb and Zn from ZPRs and soil in the simulated fluids, 3 g of particles (<30 µm) were mixed with 30 mL of each solution in 50 mL centrifuge tubes followed by lateral reciprocal shaking at 200 rpm for 6 hr. The pH, temperature, ORP and EC were measured after the experiments, these parameters were compared with those extracted using deionized water (DI) (18 MΩ cm) (Milli-Q® Integral water purification system, Merck Millipore, USA). The bioaccessible fractions (*BFs*) of Pb and Zn via ingestion or inhalation were determined using the following formula.

$$BFs\% = (C_{\text{bio}}/C_{\text{total content}})*100$$

Where, $C_{\text{bio}}$ is the concentration of the Pb and Zn in <30 µm particles via inhalation (simulated fluids) or ingestion (gastric fluids; at pH<1 or 2) and $C_{\text{total content}}$ is the total content (AR digestion/solid-phase partitioning content) of Pb and Zn in ZPRs/soil(< 250 µm particles).

### *2.4. Solid-phase partitioning for cationic element speciation*

The extraction technique utilized in this study was based on the prior research of Marumo et al. (2003) and Tessier et al. (1979). The method partitions elements of interest into five distinct phases, namely, (1) exchangeable, (2) carbonates, (3) iron and manganese oxides, (4) organic matter and sulfide minerals, and (5) residual. One gram of the ZPRs for each particle size <30 µm, 30-75 µm, 75-150 µm and 150-250 µm was mixed with different extractants for steps 1 to 5 to extract Pb/Zn elemental bound phases for each particle size. Following the predetermined extraction step, the suspension were centrifuged at 3,500 rpm for 30 minutes to segregate the leachate from the residue. For precision, all batches were conducted in triplicates, summary of the extraction procedure is shown in Table S2. Leachates from the extraction steps were analyzed using ICP-AES.

***2.5. Potential human health risk assessment***

Health risks associated with non-carcinogenic Pb and Zn from ZPRs/soil were evaluated using hazard quotient (*HQ*) risk assessment models developed by United States Environmental Protection Agency (US EPA, 2011). The models were utilized to evaluate the risks associated with inhalation and ingestion ZPRs/soil via chronic daily intake (*CDI*) in children and adults. The *HQ* was determined using *CDI* through inhalation or ingestion by the correction coefficient from simulated and gastric fluids, $C_S$ is the total content of ingestible and inhalable dust for both exposure scenarios, the formular is given by:

$$CDI_{\text{ingestion}} = \frac{(BFs)C_S \text{ x } IR_S \text{ x } EF\text{x } ED \text{ x } 10^{-6}}{BW \text{ x } AT}$$

$$CDI_{\text{inhalation}} = \frac{(BFs)C_S \text{ x } IR_D\text{x } EF \text{ x } ED}{BW \text{ x } AT\text{x } PEF}$$

$$HQ = \frac{CDI}{RfD}$$

Where, $IR_S$ is the ingestion rate (child; 200 mg/kg, adult; 100 mg/kg) (US EPA, 2011) of the ZPRs/soil and $IR_D$ is dust inhalation rate (20 mg/cm$^2$; adults and children) (US EPA, 2002). *EF* is the exposure frequency to ZPRs/soil (350 days/year; adults and children) (US EPA, 2011), *ED* refers to the exposure duration (child; 6 years, adult; 24 years)(US EPA, 2011), *BW* is the average body weight (child; 15 kg, adult; 70 kg) (US EPA, 1989), *AT* is average time for non-carcinogens exposure (*ED* x 365; child and adult) (US EPA, 2002), *PEF* is the particle emission factor ($1.36 \times 10^9$ m$^3$/kg; child and adult) (US EPA, 2002) and *RfD* is the reference dose for Pb; 0.0035 mg/kg/d, (Korre et al., 2002), Zn; 0.3 mg/kg/d (Helser et al., 2022) and $10^{-6}$ is the conversion factor (kg/mg) (US EPA, 2002).

***2.6. Quality control and geochemical modeling***

For quality control and assurance, concentrations (ranging from 0.1 to 20 mg/L) of certified reference materials traceable to NIST SRM® (Merck KGaA, Darmstadt, Germany), together with blank solutions (Millipore Milli-Rx 12α system, Merck Millipore, USA) were analyzed to determine the relative standard deviation (*RSD*) for each element. The mean and *RSD* were calculated for each element, with a margin of error of ± 2-3% and a detection limit of 0.01-0.001 mg/L. The quality assurance of analytes yielded satisfactory results, since the concentrations fell within the uncertainty range for both the certified and measured values (Table S3).

OriginPro (OriginLab Corporation, Northampton, MA 0106, USA) was used for data analysis. Thermodynamic speciation modeling for groundwater samples was carried out using Visual MINTEQ 3.1 (Gustafsson, 2011). The input dataset comprised temperature, pH, pe (calculated from ORP and temperature), alkalinity, and concentrations of Pb, Zn, Ca, Mg, Na, K, Fe, Si, and $SO_4^{2-}$. Saturation indices (*SI*s) for gastric speciation of Pb and Zn in the ZPRs under pH <1 were calculated using PHREEQC with minteq4 database (Parkhurst and Appelo, 2013). Eh-pH stability diagrams of Pb and Zn were created using the Geochemist's Workbench® (Bethke, 1992) with Thermoddem database-BRGM based on solute activities measured in the experiments.

## 3. Results and Discussion

### *3.1 Characteristics of solid samples*

The ZPRs predominantly consist of hematite ($Fe_2O_3$; 41.1wt.%), silica ($SiO_2$: 21.4wt.%), and sulfur (S; 16.2wt.%) (Fig. 2). Additionally, they also contain calcium oxide (CaO) and aluminum oxide ($Al_2O_3$) with contents of 6.7wt.% and 1.9wt.% respectively. Contents of trace elements, Pb at 7.1wt.% and Zn at 2.3wt.%, were slightly higher in comparison with the AR digestion of bulk samples, which amounted to 5.9wt.% and 1.6wt.% of Pb and Zn, respectively. Mineralogical analysis revealed that the primary mineral constituents of the ZPRs were of secondary mineralization which comprises anglesite ($PbSO_4$) and zincosite ($ZnSO_4$), accompanied by quartz ($SiO_2$) (Mufalo et al., 2023). Sulfide minerals were not detected; however, SEM observation elucidated their presence, together with Ca-bearing minerals (Fig. S3). Minor minerals include gypsum ($CaSO_4{\cdot}2H_2O$), ubiquitous goethite (FeOOH) and hematite ($Fe_2O_3$). No Pb-bearing minerals were found in the soils (S1-S8) surrounding the mine site, as reported in our previous study (Mufalo et al., 2021).

### *3.2 Influence of ZPRs on groundwater*

The groundwater sampled between 2017 to 2021 from the monitoring wells installed around the ZPRs; KA-01, KA-02 and KA-03 are shown in Fig. 3. The stiff diagram of all the sampling years for KA-01 showed a Ca-$SO_4$ type, those from KA-02 and KA-03 were mostly of Mg-$HCO_3$ and Ca-Mg-$HCO_3$ type. The Ca/Mg–$HCO_3$ groundwater type observed in KA-02 and KA-03 indicated a prevalence of alkaline earth metal ions ($Ca^{2+}$ and $Mg^{2+}$) along with weak acid/base ($HCO_3^-$). The $Ca^{2+}$ and $Mg^{2+}$ might be attributed to the dissolution of carbonates present in the bedrocks of Kabwe, specifically lithological formations such as dolomite (Kamona and Friedrich, 2007; Langman and Moberly, 2018). KA-01 showed a significant dominance of $SO_4^{2-}$ with concentration ranging from 1,290 to 5,260 mg/L (Fig. 4a) whereas those in KA-02 and KA-03 were between 181-240 mg/L and 140-384 mg/L, respectively. The high $SO_4^{2-}$(KA-01) can be linked to oxidation of sulfide minerals in the ZPRs, though not detected by XRD; since anglesite, a secondary mineral, is frequently observed in this site similar to either as an in-situ replacement of galena (Lara et al., 2018) or in well-formed crystals within cavities formed during the weathering of galena. This process occurs alongside the formation of coatings (e.g., lead hydroxide; PbOH, lead oxide; PbO, and other Pb-bearing carbonates or oxyhydroxides) on pre/or-existing phases (Bao et al., 2021; Fazli et al., 2018; Keim and Markle, 2015) that have become unstable due to oxidizing conditions of the ZPRs. The pH levels within KA-01 exhibited a range spanning from 5.0 to 6.5 (as depicted in Fig. 4b), coupled with elevated ORP values ranging between 236 and 390 mV (illustrated in Fig. S4(a)). KA-02 and KA-03 indicated a neutral pH range of 7.0 to 7.5 (Fig. 4b), which consistently displayed lower EC values (Fig. S4(b)) throughout the sampling years. The concentration of Pb in KA-01 fluctuated between 0.5 to 1.7 mg/L (Fig. 4c) with high Zn concentrations consistently between 1,210 and 1,490 mg/L (Fig. 4d). The Pb concentration in KA-02 and KA-03 were below the detection limit, indicating very low or negligible levels of Pb, meanwhile, Zn was <1 mg/L (Fig. 4d) from 2017 to 2021. Compared to the Zambian wastewater effluent standard, KA-01 exceeded the threshold limit of 0.5 and 1 mg/L for Pb and Zn respectively, whereas KA-02 and 03 were within the limits for both Pb and Zn (The Zambia Environmental Management Act, 2013).

A combined approach of thermodynamic modeling using Visual MINTEQ and Eh–pH diagram (Geochemist's Workbench®) was employed on 2021 groundwater samples. Elevated $SO_4^{2-}$ in KA-01 resulted in the subsequent precipitation of $Pb^{2+}$ and $SO_4^{2-}$ as $PbSO_4$ (Fig. S5), leading to a constrained mobility of dissolved Pb. This precipitation process accounted for 58% of the Pb speciation (Table S4); consistent with the apparent equilibrium conditions (± 0.5) for anglesite (saturation index (*SI*); -0.362) (Table S5). Cation pairing of Pb with bicarbonate (Rabadjieva et al., 2009) and the insoluble hydroxides (Table S4) had a negligible effect on the concentrations of free Pb ions in KA-01. Elevated concentrations of dissolved $Zn^{2+}$ in KA-01 were mainly enhanced due to the presence of Zn sulfates, potentially facilitated by the dissolution of zincosite (Fig. S6(a); Table S4). In the cases of KA-02 and KA-03, no detectable Pb was observed in the groundwater due to its limited mobility under neutral pH conditions (Ettler et al., 2020; Fazli et al., 2018, Mufalo et al., 2023; Soro et al., 2023; Tabelin et al., 2018, 2020). Neutral pH observed in KA-02 and KA-03 is attributed to the dissolution of carbonate minerals, resulting in lower concentrations of Zn in the groundwater surrounding the ZPRs since Zn ions sequestered and formed precipitates with carbonates (e.g., *SI* of smithsonite in KA-02; -0.147 and KA-03; -0.394) (Fig. S6(b); Table S5). The presence of Pb and Zn in ZPRs has a direct and significant impact on the underlying groundwater, causing the underlying groundwater to contain considerably higher levels of Pb and Zn than what is allowed by Zambian effluent standards. While the retention of HEs is beneficial through the formation of precipitates in the groundwater outside the ZPRs zone, any changes in the characteristics of ZPRs and the aquifer's transportation system can directly affect the quality of groundwater in the residential areas nearby.

***3.3 Bioaccessibility of Pb and Zn from ZPRs and nearby soils***

The *BFs* of Pb and Zn from the ZPRs in simulated and gastric fluids are illustrated in Fig. 5. Lead demonstrated bioaccessibility via inhalation exclusively in ALF (2.8%) and not in GS or PBS, whereas Zn was bioaccessible in ALF, GS and PBS, corresponding to *BFs* of 40, <1 and 7.4% respectively (Fig. 5a). Compared to oral intake with gastric conditions with a pH<2, higher *BFs* of Pb (12%) was observed (Fig. 5b), which further increased to 36% at pH<1. The *BFs* of Pb were lower compared to Zn, i.e., at pH<2, 50% of Zn was found to be bioaccessible and elevated to 70% at pH<1. Under extremely acidic conditions, the ZPRs exhibit a tendency to release a greater quantity of bioaccessible Zn when compared to Pb. As the pH increases >2, the solubility of Pb in the ZPRs tends to decrease faster as observed with ALF (pH 4.5). Ingestible soil (Fig. S7) showed a different trend of higher *BFs* of Pb compared Zn accounting for *BFs* of 58 to 94% (Fig. S7(a)) and 54 to 74% (Fig. S7(b)) for Pb under pH<1 and 2 respectively, whereas *BFs* of Zn ranged from 28 to 85% (pH<1) (Fig. S7(c)) and 11 to 56% (pH <2) (Fig. S7(d)), indicating an increased risk of bioaccessible Pb than Zn from the adjacent soils. In addition, the results of inhalable dust from the soil showed that Pb and Zn exhibited *BFs* only in ALF, with slightly lower *BFs* of Pb ranging from 7 to 34% to that of Zn; 8 to 43% (Fig. S7(e) and (f)). The GS and PBS extracts of the soil did not yield any detectable levels of Pb or Zn.

Both the ZPRs and soil samples displayed notable changes in ORP when exposed to ALF and PBS (Fig. S8(a)). Elevated rates of Zn in ALF compared to GS and PBS are attributed to the low pH (Fig. S8(b)), which alternatively enhanced Zn solubility compared to GS and PBS. Underlying assumptions include: 1) low driving force of Zn in the formation of complex compounds via adsorption/precipitation because of competitive interactions between exchangeable cations e.g., $Na^+$, $K^+$, $Ca^{2+}$, $Mg^{2+}$ and $Zn^{2+}$ present in the solution, particularly at pH<7 (Metwally et al., 1993); 2) increase in proton-promoted dissolutions of Zn-bearing minerals coupled with desorption from complexes, e.g., iron oxyhydroxides/oxides and carbonates (Bao et al., 2021; Cardoso et al., 2021). At pH>7 complexes with $OH^-$ i.e., Zn $(OH)_2$, Zn $(OH)_3^-$ and Zn $(OH)_4^{2-}$ (Metwally et al., 1993; Kaya and Ören, 2005) promote adsorption and precipitation within the solution. The reduced bioaccessible Pb in ALF and undetected Pb in GS and PBS may be explained by the decreased mobility of Pb in the pH range of 4 to 8 (Tabelin et al., 2018). Under circum-neutral conditions, where the pH is 7.3 (observed in both GS and PBS), the potential arises for the co-precipitation of Pb alongside specific organic compounds present in simulated fluids (listed in Table S1). The concurrent precipitation has the potential to impede the mobility of Pb. Guney et al. (2017) observed a comparable pattern in both soils and mine tailings. They reported higher *BFs* of Pb and Zn extracted from particles <20 µm using ALF, as opposed to GS. Considering dust particles <30 µm originating from ZPRs and the adjacent soils, the limited *BFs* of Pb in simulated fluids, particularly ALF, indicate that the likelihood of Pb phagocytosis is improbable until significant dissolution occurs. Consequently, the bioaccessible Pb, which could potentially lead to its bioavailability in the body, poses a low risk if inhaled.

### *3.4 Cationic speciation of Pb and Zn in varying particles sizes of the ZPRs*

Cationic speciation of Pb (a) and Zn (b) in ZPRs for particle sizes (<30 µm, 30-75 µm, 75-150 µm, 150-250 µm) and *BFs*/phases at pH<1 and 2 is presented in Fig. 6. The *BFs* of Pb were mainly from “geochemically labile phases" i.e., exchangeable + carbonates+ Fe/Mn oxide phases at pH<1(Fig. 6(a)). Distribution of Pb-bound phases in particles <30 µm and those ranging from 30 to 75 µm indicated a slightly higher proportion of labile fractions at 32%, in contrast to 27% observed in particles ranging from 75 to 150 µm and 150 to 250 µm. This could be attributed to the reduced particle size of <30 µm and 30 to 75 µm which enhances the proportion and/or surface area of the sorbent phase, i.e., Pb bound in mineralized secondary sulfates, e.g., anglesite (Fazli et al., 2018), carbonates or adsorbed to Fe-oxyhydroxides. Regardless of the partitioning fractions, chemical-bound phases of Pb dissolve ca. 31 to 37% for (< 30 µm, 30-75 µm, 75-150 µm, 150-250 µm) (Fig. 6(a); Table S6), with a distinct resemblance in the *BFs* for particles <30 µm (34%) and those within the range of 75-150 µm (35%). Particles in the range 30 to 75 µm exhibited higher bioaccessible Pb (37%), whereas the lowest was in the 150 to 250 µm size range. This shows that segregated ZPRs based on distinct particle size ranging from 0 to <150 µm, pose a notable and increased potential for bioaccessible Pb under pH<1 from the labile phases. In contrast, figure 6(b) indicates that Zn displayed a different trend, with lower Zn-bound fractions in the labile phases of <30 µm (31%) and 30-75 µm (32%) compared to 75-150 µm (34%) and 150- 250 µm (36%) size fractions. The higher fractions in 75-150 µm and 150-250 µm particles might be due to encapsulation of soluble phases from smaller particles, e.g., zincosite into the larger particles (Cardoso et al., 2021; Kim et al., 2011). This contributes to a higher labile fraction of Zn in particles within the size range of 75-150 µm and 150-250 µm.

Bioaccessible fractions of Pb were reduced to 11% at pH<2 (Fig. 6(a); Table S7) which indicated *BFs* predominately from the exchangeable phase for <30 µm and 30-75 µm particles and to some extent exchangeable/carbonate phase for 75-150 µm and 150- 250 µm particles. Dissolution of all labile Zn phases was apparent at both pH<1 and 2 probably due to enhanced Zn solubility (Fig. 6(b); Table S7) (Khan et al. 2022; Tabelin et al., 2020). While phases containing Pb/Zn dissolve/become bioaccessible at low pH (as shown in Table S8), the dissolution kinetics at elevated pH (Ruby et al., 1992), significantly contribute to Pb bioaccessibility. For example, encapsulation of Pb-bearing surfaces by weathering rinds, inert phases (such as silicates; Fig S3), and precipitation products (Langman and Moberly, 2018), leading to a slow dissolution process (Helser et al., 2022; Meng et al., 2018). This aligns with the typical behavior of Pb in the ZPRs, since it predominantly exists in phases that are resistant to chemical weathering and remain insoluble, e.g., as residues (49-50%) and oxidizable phases (17-23%), as those phase fractions persist throughout the dissolution process. Zinc demonstrated instability, elucidating the heightened dissolution characterized by a partitioning sequence of residues > exchangeable > Fe/Mn oxide> sulfide/organic matter> carbonates.

Lead (8-11%) and Zn (11-13%) in the reducible phase were likely occluded with Fe-oxyhydroxides, e.g., gothite (FeOOH) observed in XRD, supported by the pervasive Fe in the SEM-EDS (Fig.S3). Moreover, ZPRs exhibit negligible Fe release via batch leaching, as reported by Tangviroon et al. (2020). Dissolution of Fe-oxyhydroxides becomes pivotal in the release of Pb and Zn under highly oxidizing conditions. The Zn bound to weak acid soluble (up to 5%) were not significant compared to Pb (7-13%). Carbonate-bound fractions could be attributed to cerussite (Lara et al., 2018; Fazli et al., 2018); also occurs as a weathering product of galena, although not detected by XRD. According to Helser et al. (2022), higher bioaccessible Pb is anticipated to originate from the dissolution of Pb carbonates. The in vivo gastric studies on sulfide tailings revealed that Pb carbonates exhibited significantly higher

Pb bioaccessibility compared to Pb associated with Fe-oxyhydroxides or sulfides. Bioaccessible Pb and Zn released from the labile phases of ZPRs under pH 1 and 2 may pose a significant risk of intoxication within the human body. This potential hazard underscores the serious threat posed by the ingestion of these mine wastes.

### *3.5 Environmental health hazard implications*

Associated risks with bioaccessible Pb and Zn originating from ZPRs and soils through inhalation and ingestion by both adults and children are provided in Tables S9 and S10. The hazard quotients (*HQ*) for the ingestion of Pb from ZPRs were found to be elevated, reaching up to 230 for children and up to 25 for adults (*HQ* >>>>1) (Table S9). Despite considering the correction coefficient applied to *HQ* ($HQ_h$ and $HQ_g$) to simulate ingestion risks with gastric pH conditions of <1 and 2; the results indicate that both children and adults remain susceptible to Pb intoxication from the ingestion of ZPRs. It is noteworthy that no Zn intoxication risks were observed from the ZPRs, despite Zn demonstrating higher *BFs* in simulated and gastric fluids, *HQ* for both adults and children were <<<1 (Table S9). In addition, the findings suggest that there was a lower risk associated with inhaling Pb or Zn from ZPRs (Table S10). When considering potential hazards stemming from the surrounding soils, Fig. 7 demonstrates that the risks associated with Pb ingestion are linked to the consumption of soil in close proximity to the legacy mine. The *HQ* in the vicinity of the mine site indicated values >1 for ingestion of soil with children being the most susceptible even at gastric ingestion conditions of pH<2 (Fig. 7(b)). Children are particularly receptive to both scenarios of hazard evaluation ($HQ_h$ and $HQ_g$) probably due to their higher gastrointestinal adsorption and tendency to engage in pica (Bello et al., 2016) both of which contribute to elevated levels of Pb in their bodies. The outcomes of this study provide compelling evidence regarding the pathway of Pb intoxication in Kabwe, which is largely attributed to ingestible mine wastes or contaminated soils and dust. Whether done intentionally or accidentally, or even ingested with food, it's crucial to exercise caution and mindfulness when consuming meals. Equally important is raising awareness among parents to vigilantly supervise their children during playtime (Mufalo et al., 2021), in order to prevent pica behavior. Our earlier research has put forth suggestions for remediating ZPRs (Mufalo et al., 2023; Tangviroon et al., 2020) in order to avert contamination of groundwater and dispersion of aerosols. This undertaking gains even greater urgency from the findings of this study, underscoring the imperative for swift action in addressing the environmental legacy of the Kabwe mine.

## 4. Conclusion

This study aimed to assess the influence of ZPRs on the underlying groundwater and the bioaccessible fractions of Pb and Zn released from the ZPRs. Additionally, the study explored potential exposure routes and hazard evaluation including nearby soils of the mine site in Kabwe, Zambia. The key findings of this investigation can be summarized as follows:

1) ZPRs directly impacted the underlying groundwater, with Pb and Zn concentrations surpassing the Zambia wastewater effluent standard. However, retention of Zn in the surrounding groundwater is attributed to the formation of carbonate precipitates like smithsonite.

2) Bioaccessible Pb resulting from inhalation of <30 µm of ZPRs and the surrounding soils is lower compared to bioaccessible Pb from ingestion of <250 µm ZPRs/soil particles.

3) Bioaccessible Pb is ascribed to the dissolution of Pb-bound phases in the ZPRs, and it is significantly influenced by the pH level under gastric conditions. A pH<1 promotes the dissolution of Pb/Zn bound phases in the labile fractions, i.e., exchangeable, carbonate and Fe/Mn oxides. However, at pH<2, only the exchangeable/carbonate bound Pb phases become bioaccessible.

4) Solid-phase partitioning suggests that particle size influence bioaccessible Pb in the ZPRs labile phases of <30 µm, 30-75 µm, 75-150 µm, 150-250 µm particles. Higher bioaccessible Pb is attributed to dissolution labile Pb-bound phases in <30-75 µm particles.

5) The hazard quotient indicated that ZPRs present non-carcinogenic hazards for both adults and children in relation to Pb exposure. Whereas Zn exhibited higher bioaccessible fractions, the non-carcinogenic consequences were negligible.

6) Ingestion of soil in the vicinity of the legacy mine revealed elevated risks of Pb intoxication. Notably, among the residents susceptible to Pb intoxication, children are the most vulnerable.

**Acknowledgment**

This work was supported by JST/JICA SATREPS (Science and Technology Research Partnership for Sustainable Development; No. JPMJSA1501) and aXis (Accelerating Social Implementation for SDGs Achievement; No. JPMJAS2001) funded by JST for the financial support and JST AJ-CORE Project, JSPS CORE to CORE program, Hokkaido University SOUSEI-TOKUTEI Specific Research Projects, and Grants-in-Aid for Scientific Research from the Ministry of Education, Culture, Sports, Science and Technology of Japan. The authors also wish to thank Dr. Shuji Tamamura and Dr. Takuma Murakami of Horonobe Research Institute for the Subsurface Environment for their assistance during the XRD and XRF analysis of the samples.

**Authorship contribution statement**

**Walubita Mufalo**; Conceptualization; Formal analysis; Investigation; Methodology; Writing - original draft; Writing - review & editing. **Takahiko Arima**; Formal analysis; Validations; Writing - review & editing. **Toshifumi Igarashi**; Conceptualization, Supervision; Methodology; Formal analysis; Validations; Writing-review & editing. **Mayumi Ito, Tsutomu Sato, Shingo Tomiyama, Imasiku Nyambe**, **Carlito Baltazar Tabelin**; Resources; Writing-review & editing. **Hokuto Nakata, Shouta Nakayama, Mayumi Ishizuka**; Project administration; Funding acquisition; Writing-review & editing.

**References**

Abraham, J., Dowling, K., Florentine, S. (2018). Assessment of potentially toxic metal contamination in the soils of a legacy mine site in Central Victoria, Australia. *Chemosphere, 192*, 122-132.

Arenas-Lago, D., Lago-Vila, M., Rodríguez-Seijo, A., Andrade, M.L., Vega, F.A. (2014). Risk of metal mobility in soils from a Pb/Zn depleted mine (Lugo, Spain). *Environmental Earth Science, 72(7)*, 2541-2556.

Baieta, R., Mihaljevič, M., Ettler, V., Vaněk, A., Penížek, V., Trubač, J., Kříbek, B., Ježek, J., Svoboda, M., Sracek, O., Nyambe, I. (2021). Depicting the historical pollution in a Pb–Zn mining/smelting site in Kabwe (Zambia) using tree rings. *Journal of African Earth Sciences, 181*, 104246.

Bao, Z., Al, T., Couillard, M., Poirier, G., Bain, J., Shrimpton, H.K., Finfrock, Y.Z., Lanzirotti, A., Paktunc, D., Saurette, E., Hu, Y. (2021). A cross scale investigation of galena oxidation and controls on mobilization of lead in mine waste rock. *Journal of Hazardous Material, 412*, 125130.

Behrooz, R.D., Kaskaoutis, D.G., Grivas, G., Mihalopoulos, N. (2021). Human health risk assessment for toxic elements in the extreme ambient dust conditions observed in Sistan, Iran. *Chemosphere, 262*, 127835.

Bello, O., Naidu, R., Rahman, M.M., Liu, Y., Dong, Z. (2016). Lead concentration in the blood of the general population living near a lead–zinc mine site, Nigeria: Exposure pathways. *Science of Total Environment, 542*, 908-914.

Bethke, C. (1992). The Geochemist's Workbench: *A Users Guide to Rxn, Act2, Tact, React, and Gtplot.* C. Bethke.

Boisa, N., Elom, N., Dean, J.R., Deary, M.E., Bird, G., Entwistle, J.A. (2014). Development and application of an inhalation bioaccessibility method (IBM) for lead in the PM10 size fraction of soil. *Environment International, 70*, 132-142.

Caboche, J., Esperanza, P., Bruno, M., Alleman, L.Y. (2011). Development of an in vitro method to estimate lung bioaccessibility of metals from atmospheric particles. *Journal of Environmental Monitoring, 13(3)*, 621-630.

Cardoso, D., Narcy, A., Durosoy, S., Bordes, C., Chevalier, Y. (2021). Dissolution kinetics of zinc oxide and its relationship with physicochemical characteristics. *Powder Technology, 378*, 746-759.

Charlatchka, R., Cambier, P. (2000). Influence of reducing conditions on solubility of trace metals in contaminated soils. *Water Air Soil Pollution, 118*,143-168.

Concas, A., Ardau, C., Cristini, A., Zuddas, P., Cao, G. (2006). Mobility of heavy metals from tailings to stream waters in a mining activity contaminated site. *Chemosphere, 63(2)*,244-253.

Coynel, A., Schäfer, J., Dabrin, A., Girardot, N., Blanc, G. (2007). Groundwater contributions to metal transport in a small river affected by mining and smelting waste. *Water Research, 41(15)*, 3420-3428.

Ettler, V., Cihlová, M., Jarošíková, A., Mihaljevič, M., Drahota, P., Kříbek, B., Vaněk, A., Penížek, V., Sracek, O., Klementová, M., Engel, Z. (2019). Oral bioaccessibility of metal (loid) s in dust materials from mining areas of northern Namibia. *Environment Intentional, 124*, 205-215.

Ettler, V., Štěpánek, D., Mihaljevič, M., Drahota, P., Jedlicka, R., Kříbek, B., Vaněk, A., Penížek, V., Sracek, O., Nyambe, I. (2020). Slag dusts from Kabwe (Zambia): Contaminant mineralogy and oral bioaccessibility. *Chemosphere, 260*, 127642.

Expósito, A., Markiv, B., Ruiz-Azcona, L., Santibáñez, M., Fernández-Olmo, I. (2021). Understanding how methodological aspects affect the release of trace metal (loid) s from urban dust in inhalation bioaccessibility tests. *Chemosphere, 267*, 129181.

Fazli, S., Taghipour, B., Lentz, D.R. (2018). The Zn-Pb sulfide and Pb-Zn-Ag non-sulfide Kuh-e-Surmeh ore deposit, Zagros Belt, Iran: Geologic, mineralogical, geochemical, and S isotopic constraints. *Journal of Geochemical Exploration,194*, 146-166.

Guney, M., Bourges, C.M.J., Chapuis, R.P., Zagury, G.J. (2017). Lung bioaccessibility of As, Cu, Fe, Mn, Ni, Pb, and Zn in fine fraction (< 20 μm) from contaminated soils and mine tailings. *Science of Total Environment, 579*, 378-386.

Gustafsson, J.P. (2011). Visual MINTEQ 3.0 user guide. KTH, Department of Land and Water Recources, Stockholm, Sweden, 550.

Helser, J., Vassilieva, E., Cappuyns, V. (2022). Environmental and human health risk assessment of sulfidic mine waste: Bioaccessibility, leaching and mineralogy. *Journal Hazardous. Materials, 424*, 127313.

Kamona, A.F., Friedrich, G.H. (2007). Geology, mineralogy and stable isotope geochemistry of the Kabwe carbonate-hosted Pb–Zn deposit, Central Zambia. *Ore Geology Reviews, 30(3-4),* 217-243.

Kastury, F., Smith, E., Juhasz, A.L. (2017). A critical review of approaches and limitations of inhalation bioavailability and bioaccessibility of metal (loid) s from ambient particulate matter or dust. *Science of Total Environment, 574*, 1054-1074.

Kaya, A., Ören, A.H. (2005). Adsorption of zinc from aqueous solutions to bentonite. *Journal of Hazardous Materials, 125(1-3)*, 183-189.

Keim, M.F., Markl, G. (2015). Weathering of galena: Mineralogical processes, hydrogeochemical fluid path modeling, and estimation of the growth rate of pyromorphite. *American Mineralogist, 100(7)*, 1584-1594.

Khan, Y.K., Toqeer, M., Shah, M.H. (2022). Mobility, bioaccessibility, pollution assessment and risk characterization of potentially toxic metals in the urban soil of Lahore, Pakistan. *Environmental Geochemistry Health*, 1-22.

Khelifi, F., Caporale, A.G., Hamed, Y., Adamo, P. (2021). Bioaccessibility of potentially toxic metals in soil, sediments and tailings from a north Africa phosphate-mining area: Insight into human health risk assessment. *Journal of Environmental Management*, 279, 111634.

Khoeurn, K., Sakaguchi, A., Tomiyama, S., Igarashi, T. (2019). Long-term acid generation and heavy metal leaching from the tailings of Shimokawa mine, Hokkaido, Japan: Column study under natural condition. *Journal of Geochemical Exploration*, 201, 1-12.

Kim, C.S., Wilson, K.M., Rytuba, J.J. (2011). Particle-size dependence on metal (loid) distributions in mine wastes: Implications for water contamination and human exposure. *Applied Geochemistry, 26(4)*, 484-495.

Kok, J.F., Parteli, E.J., Michaels, T.I., Karam, D.B. (2012). The physics of wind-blown sand and dust. *Reports on Progress in Physics, 75(10)*, 106901.

Korre, A., Durucan, S. and Koutroumani, A. (2002). Quantitative-spatial assessment of the risks associated with high Pb loads in soils around Lavrio, Greece. *Applied Geochemistry, 17(8)*, 1029-1045.

Kříbek, B., Nyambe, I., Majer, V., Knésl, I., Mihaljevič, M., Ettler, V., Vaněk, A., Penížek, V., Sracek, O. (2019). Soil contamination near the Kabwe Pb-Zn smelter in Zambia: Environmental impacts and remediation measures proposal. *Journal of Geochemical Exploration, 197*, 159-173.

Langman, J.B., Moberly, J.G. (2018). Weathering of a mined quartz-carbonate, galena-sphalerite ore and release and transport of nanophase zinc carbonate in circumneutral drainage. *Journal of Geochemical Exploration,188*, 185-193.

Lara, R.H., Briones, R., Monroy, M.G., Mullet, M., Humbert, B., Dossot, M., Naja, G.M., Cruz, R. (2011). Galena weathering under simulated calcareous soil conditions. *Science of Total Environment, 409(19)*, 3971-3979.

Li, X., Gao, Y., Zhang, M., Zhang, Y., Zhou, M., Peng, L., He, A., Zhang, X., Yan, X., Wang, Y., Yu, H. (2020). In vitro lung and gastrointestinal bioaccessibility of potentially toxic metals in Pb-contaminated alkaline urban soil: The role of particle size fractions. *Ecotoxicology and Environmental Safety, 190*, 110151.

Li, Y., Padoan, E. and Ajmone-Marsan, F. (2021). Soil particle size fraction and potentially toxic elements bioaccessibility: A review. *Ecotoxicology Environmental Safety, 209*, 111806.

Marove, C.A., Sotozono, R., Tangviroon, P., Tabelin, C.B., Igarashi, T. (2022). Assessment of soil, sediment and water contaminations around open-pit coal mines in Moatize, Tete province, Mozambique. *Environmental Advances, 8*, 100215.

Marumo, K., Ebashi, T., Ujiie, T. (2003). Heavy metal concentrations, leachabilities, and lead isotope ratios of Japanese soils. *Shigen-Chihsitsu*, 53, 125-146.

Meng, J., Tao, M., Wang, L., Liu, X., Xu, J. (2018). Changes in heavy metal bioavailability and speciation from a Pb-Zn mining soil amended with biochars from co-pyrolysis of rice straw and swine manure. *Science of Total Environment, 633*, 300-307.

Metwally, A.I., Mashhady, A.S., Falatah, A.M., Reda, M. (1993). Effect of pH on zinc adsorption and solubility in suspensions of different clays and soils. *Zeitschrift für Pflanzenernährung und Bodenkunde*, 156(2), 131-135.

Mufalo, W., Tangviroon, P., Arima, T., Igarashi, T., Ito, M., Sato, T., Noto, K., Kawashima, T., Nyambe, I., Nakata, H., Nakayama, S., Ishizuka, M. (2023). Immobilization of Pb and Zn leached from mining residue materials in Kabwe, Zambia: Performance of calcined dolomite in column experiments. *Journal of Geochemical Exploration, 249*, 107209.

Mufalo, W., Tangviroon, P., Igarashi, T., Ito, M., Sato, T., Chirwa, M., Nyambe, I., Nakata, H., Nakayama, S., Ishizuka, M. (2021). Solid-phase partitioning and leaching behavior of Pb and Zn from playground soils in Kabwe, Zambia. *Toxics, 9(10*), 248.

Nakamura, S., Igarashi, T., Uchida, Y., Ito, M., Hirose, K., Sato, T., Mufalo, W., Chirwa, M., Nyambe, I., Nakata, H., Nakayama, S., Ishizuka, M. (2021). Evaluation of dispersion of lead-bearing mine wastes in Kabwe District, Zambia. *Minerals, 11(8)*, 901.

Nakamura, S., Igarashi, T., Uchida, Y., Ito, M., Hirose, K., Sato, T., Mufalo, W., Chirwa, M., Nyambe, I., Nakata, H., Nakayama, S., Ishizuka, M. (2022). Impacts of surface water on windborne lead dispersion from the zinc plant residue in Kabwe, Zambia. *Minerals, 12(5)*, 535

Nakata, H., Nakayama, S.M., Yabe, J., Muzandu, K., Kataba, A., Ikenaka, Y., Ishizuka, M. (2022). Interdisciplinary approach to addressing lead pollution caused by mining activity in Kabwe, The Republic of Zambia. *Environmental Monitoring and Contaminants Research*, *2*, 94-111

Nakata, H., Nakayama, S.M., Yabe, J., Muzandu, K., Toyomaki, H., Yohannes, Y.B., Kataba, A., Zyambo, G., Ikenaka, Y., Choongo, K., Ishizuka, M. (2021). Clinical biochemical parameters associated with the exposure to multiple environmental metals in residents from Kabwe, Zambia. *Chemosphere, 262*, 127788.

Nakayama, S.M., Ikenaka, Y., Hamada, K., Muzandu, K., Choongo, K., Teraoka, H., Mizuno, N., Ishizuka, M. (2011). Metal and metalloid contamination in roadside soil and wild rats around a Pb–Zn mine in Kabwe, Zambia. *Environmental Pollution,159(1)*, 175-181.

Nishimoto, N., Yamamoto, Y., Yamagata, S., Igarashi, T., Tomiyama, S. (2021). Acid Mine Drainage Sources and Impact on Groundwater at the Osarizawa Mine, Japan. *Minerals, 11(9)*, 998.

Parkhurst, D.L. and Appelo, C.A.J. (2013). Description of input and examples for PHREEQC version 3, a computer program for speciation, batch-reaction, one-dimensional transport, and inverse geochemical calculations. US geological survey techniques and methods. 6(A43), 497.

Pelfrêne, A., Cave, M.R., Wragg, J., Douay, F. (2017). In vitro investigations of human bioaccessibility from reference materials using simulated lung fluids. *International Journal of Environmental Research and Public Health, 14(2)*, 112.

Pelfrene, A., Sahmer, K., Waterlot, C., Glorennec, P., Douay, F., Le Bot, B. (2020). Evaluation of single-extraction methods to estimate the oral bioaccessibility of metal (loid) s in soils. *Science of Total Environment, 727*, 138553.

Rabadjieva, D., Tepavitcharova, S., Todorov, T., Dassenakis, M., Paraskevopoulou, V. , Petrov, M. (2009). Chemical speciation in mining affected waters: the case study of Asarel-Medet mine. *Environmental Monitoring and Assessment,159*, 353-366.

Reyes, A., Cuevas, J., Fuentes, B., Fernandez, E., Arce, W., Guerrero, M. and Letelier, M.V. (2021). Distribution of potentially toxic elements in soils surrounding abandoned mining waste located in Taltal, Northern Chile. *Journal of Geochemical Exploration, 220*, 106653.

Ruby, M.V., Davis, A., Kempton, J.H., Drexler, J.W. and Bergstrom, P.D. (1992). Lead bioavailability-dissolution kinetics under simulated gastric conditions. *Environmental Science and Technology, 26(6)*, 1242-1248.

Singh, K. N., Narzary, D. (2021). Geochemical characterization of mine overburden strata for strategic overburden-spoil management in an opencast coal mine. *Environmental Challenges. 3*, 100060.

Soltani, N., Keshavarzi, B., Moore, F., Cave, M., Sorooshian, A., Mahmoudi, M.R., Ahmadi, M.R., Golshani, R. (2021). In vitro bioaccessibility, phase partitioning, and health risk of potentially toxic elements in dust of an iron mining and industrial complex. *Ecotoxicology and Environmental Safety, 212*, 111972.

Soro, A.T., Mufalo, W., Arima, T., Tabelin, C.B., Igarashi, T. (2023). Geochemical Characterization of Rock Samples from Selected Fiji Mine Sites to Evaluate On-Site Environmental Vulnerabilities. *Minerals, 13(5)*, 661.

Sungur, A., Soylak, M., Ozcan, H., 2014. Investigation of heavy metal mobility and availability by the BCR sequential extraction procedure: relationship between soil properties and heavy metals availability. *Chemical Speciation Bioavailability, 26(4)*, 219-230.

Tabelin, C.B., Igarashi, T., Villacorte-Tabelin, M., Park, I., Opiso, E.M., Ito, M., Hiroyoshi, N. (2018). Arsenic, selenium, boron, lead, cadmium, copper, and zinc in naturally contaminated rocks: A review of their sources, modes of enrichment, mechanisms of release, and mitigation strategies. *Science of Total Environment, 645*, 1522-1553.

Tabelin, C.B., Silwamba, M., Paglinawan, F.C., Mondejar, A.J.S., Duc, H.G., Resabal, V.J., Opiso, E.M., Igarashi, T., Tomiyama, S., Ito, M., Hiroyoshi, N. (2020). Solid-phase partitioning and release-retention mechanisms of copper, lead, zinc and arsenic in soils impacted by artisanal and small-scale gold mining (ASGM) activities. *Chemosphere, 260*, 127574.

Tangviroon, P., Noto, K., Igarashi, T., Kawashima, T., Ito, M., Sato, T., Mufalo, W., Chirwa, M., Nyambe, I., Nakata, H, Nakayama, S., Ishizuka, M. (2020). Immobilization of lead and zinc leached from mining residual materials in Kabwe, Zambia: Possibility of chemical immobilization by dolomite, calcined dolomite, and magnesium oxide. *Minerals, 10(9)*, 763.

Tembo, B.D., Sichilongo, K., Cernak, J. (2006). Distribution of copper, lead, cadmium and zinc concentrations in soils around Kabwe town in Zambia. *Chemosphere, 63(3)*, 497-501.

Tessier, A., Campbell, G.C., Bisson, M. (1979). Sequential extraction procedure for the speciation of particulate trace metals. *Analytical Chemistry, 51*, 844-851

The Environment Management Act. The environment management (licensing) regulations. SI Govt. Zambia 2013. 112, 737-858.

Tomiyama, S., Igarashi, T. (2022). The potential threat of mine drainage to groundwater resources. *Current Opinions Environmental Science and health*. 27, 100347.

Tomiyama, S., Igarashi, T., Tabelin, C.B., Tangviroon, P., Ii, H. (2019). Acid mine drainage sources and hydrogeochemistry at the Yatani mine, Yamagata, Japan: A geochemical and isotopic study. *Journal of Contaminant Hydrology, 225*, 103502.

Toyomaki, H., Yabe, J., Nakayama, S.M., Yohannes, Y.B., Muzandu, K., Liazambi, A., Ikenaka, Y., Kuritani, T., Nakagawa, M., Ishizuka, M. (2020). Factors associated with lead (Pb) exposure on dogs around a Pb mining area, Kabwe, Zambia. *Chemosphere, 247*, 125884.

US EPA. (1989). Office of Emergency and Remedial Response. Risk Assessment Guidance for Superfund: pt. A. Human health evaluation manual (Vol. 1). Office of Emergency and Remedial Response.

US EPA. (2000). Short Sheet: TRW Recommendations for Sampling and Analysis of Soil at Lead (Pb) Sites. U.S. Environmental Protection Agency, Office of Solid Waste and Emergency Response: Washington, DC. EPA 540-F-00-010. OSWER 9285, 7-38.

US EPA. (2002). Supplemental guidance for developing soil screening levels for superfund sites. United States Environ. Prot. Agency, 12, 1-187.

US EPA. (2011). Exposure factors handbook 2011 edition. US Environmental Protection Agency.

Weggeberg, H., Benden, T.F., Steinnes, E., Flaten, T.P. (2019). Element analysis and bioaccessibility assessment of ultrafine airborne particulate matter (PM0.1) using simulated lung fluid extraction (artificial lysosomal fluid and Gamble's solution). *Environmental Chemistry and Ecotoxicology,1*, 26-35.

Wiseman, C.L., Zereini, F. (2014). Characterizing metal (loid) solubility in airborne PM10, PM2. 5 and PM1 in Frankfurt, Germany using simulated lung fluids. *Atmospheric Environment. 89*, 282-289.

Yabe, J., Nakayama, S.M., Nakata, H., Toyomaki, H., Yohannes, Y.B., Muzandu, K., Kataba, A., Zyambo, G., Hiwatari, M., Narita, D., Hangoma, P., Munyinda, S.N., Mufune, T., Choongo, K., Ikenaka, Y., Yamada, D., Ishizuka, M. (2020). Current trends of blood lead levels, distribution patterns and exposure variations among household members in Kabwe, Zambia. *Chemosphere, 243*, 125412.

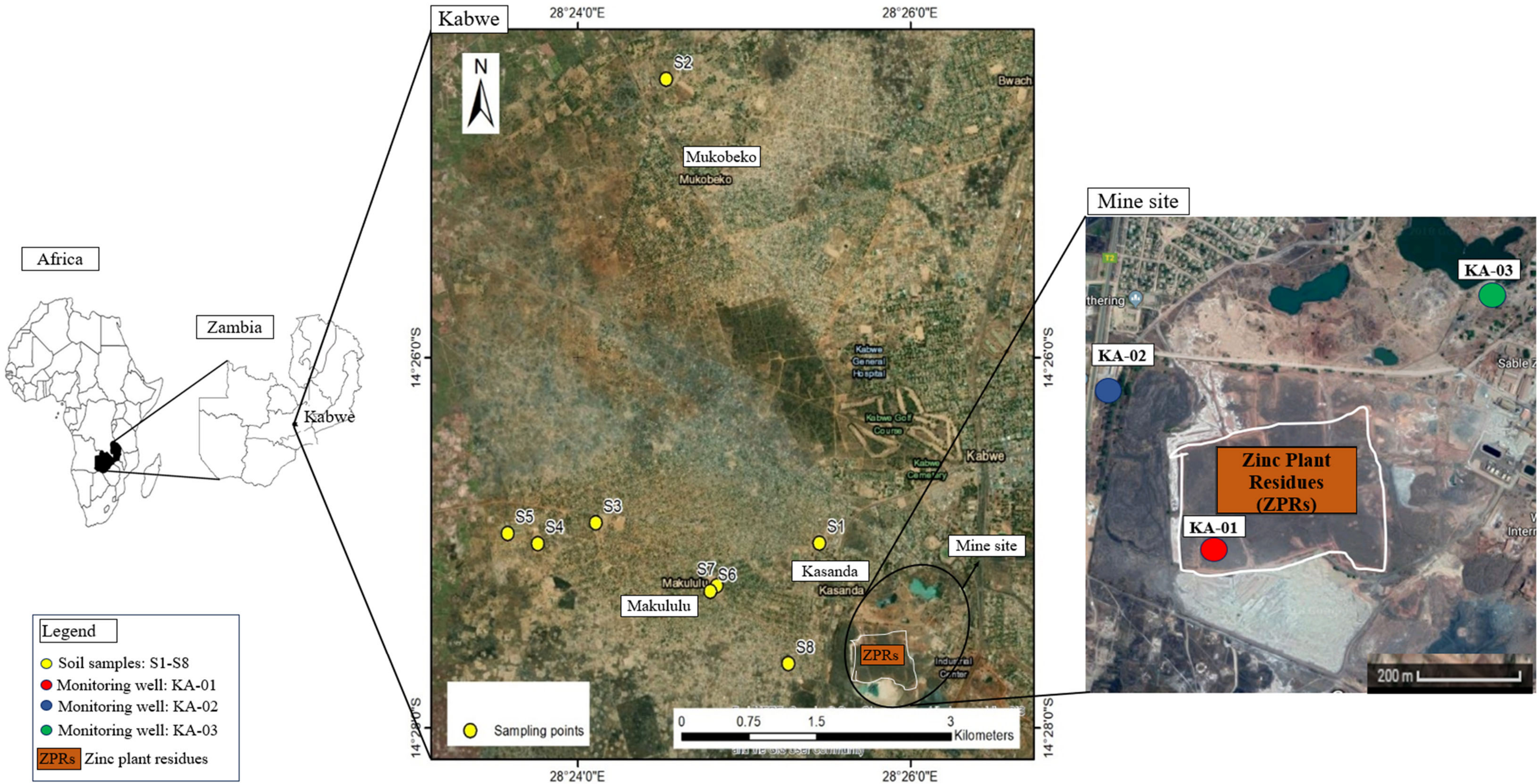


Fig. 1. Sampling location of the Zinc plant residues (ZPRs), groundwater monitoring wells in and around the ZPRs (KA-01, KA-02 and KA-03) and surrounding soils (S1 to S8) located within a 10 km (approx. 6.2 miles) radius of the mine site.

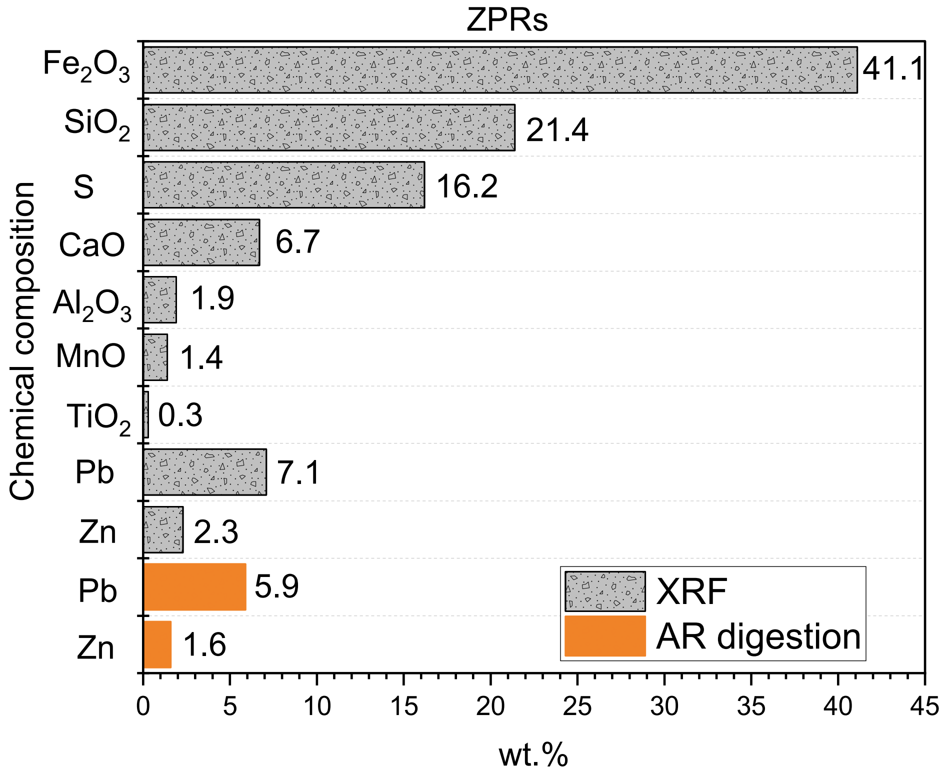


Fig. 2. Chemical composition of the ZPRs, including total contents of Pb and Zn in wt.%.

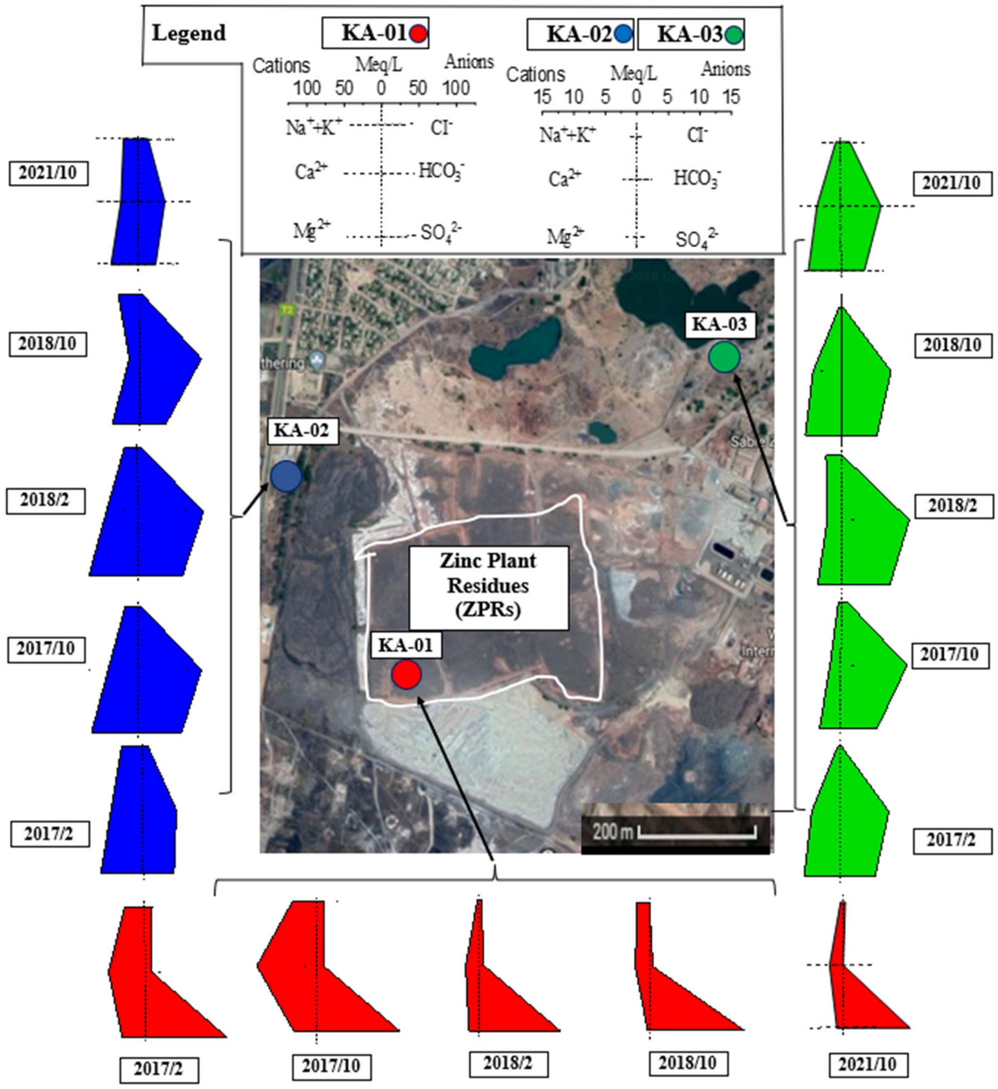


Fig. 3. Stiff of the underlaying groundwater of ZPRs from monitoring well KA-01 and outside the ZPRs KA-02 and KA-03.

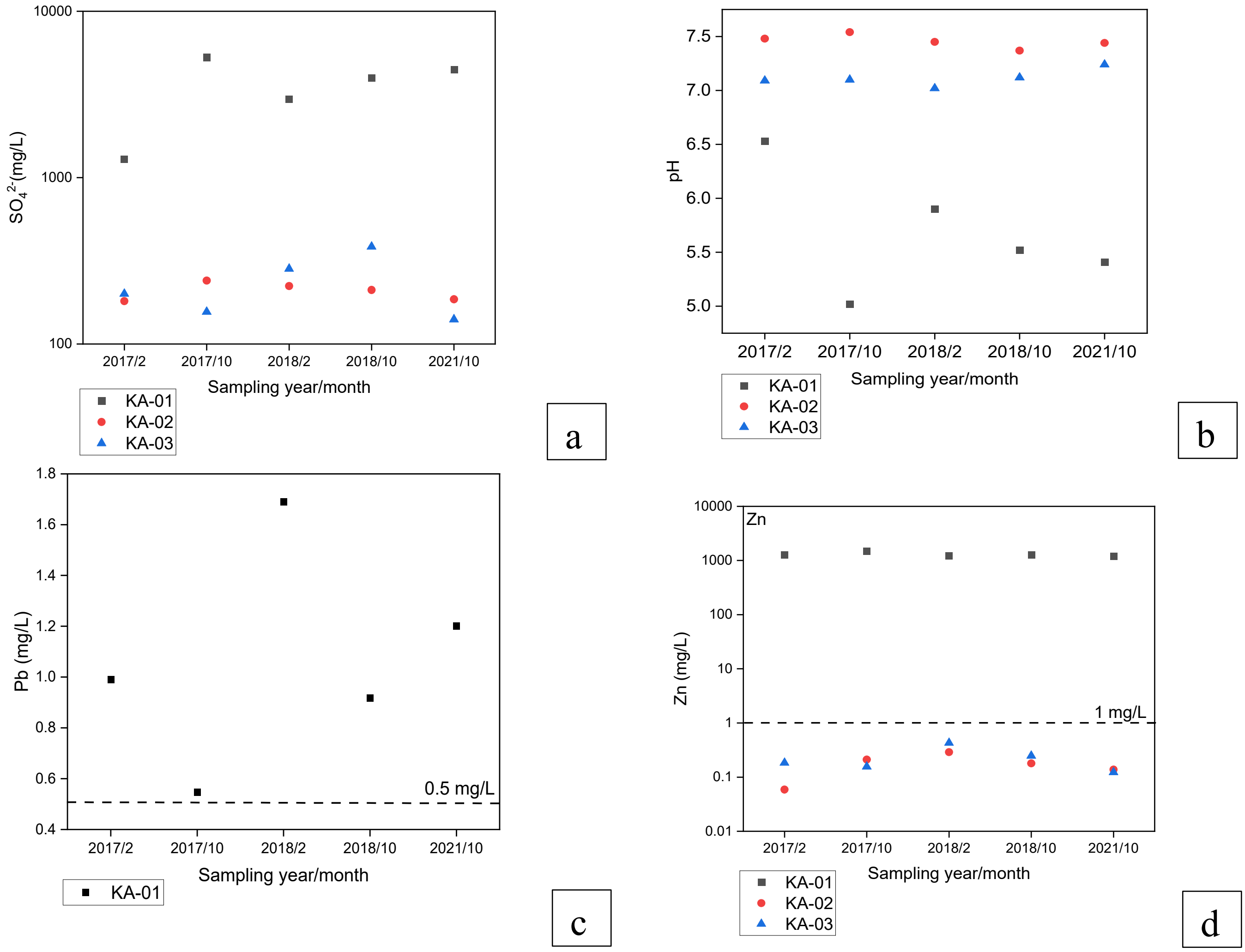


Fig. 4. Groundwater parameters of the monitoring wells KA-01, KA-02 and KA-03; (a) $SO_4^{2-}$ concentration, (b) pH, (c) Pb concentration and (d) Zn concentrations. The data line represents Zambia wastewater and effluent standard for Pb (0.5 mg/L) and Zn (1 mg/L).

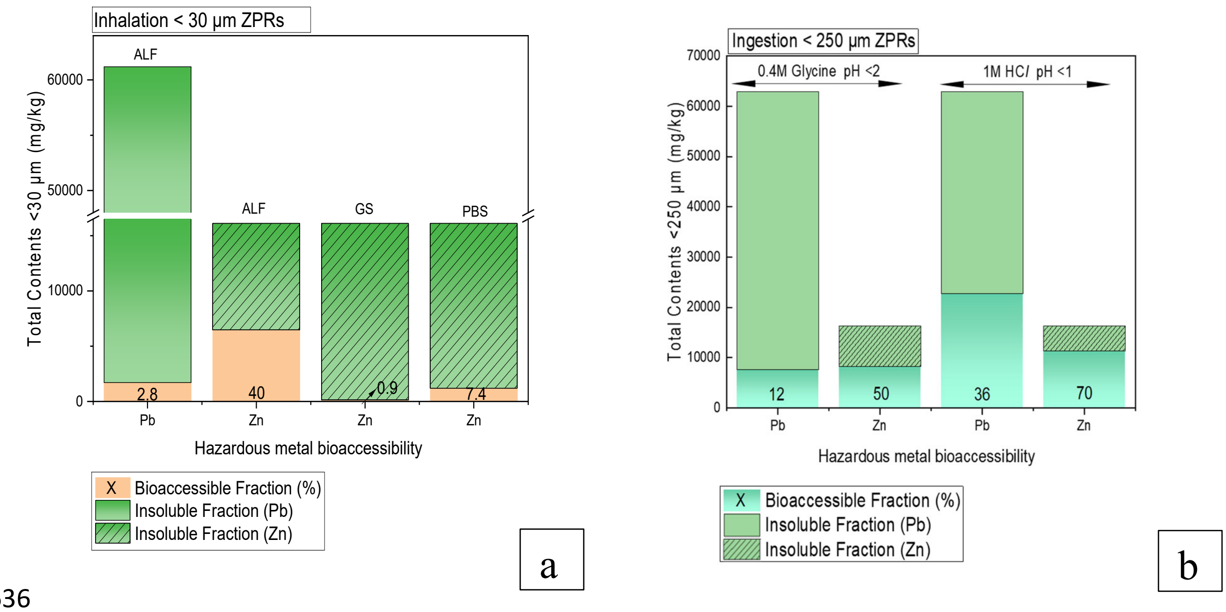


Fig. 5. Bioaccessible fractions of Pb and Zn from inhalable ZPRs particles (<30 µm) in simulated fluids (a) ALF- artificial lysosomal fluid, GS-Gamble solution, PBS-phosphate-buffered saline and (b) Bioaccessible fractions of Pb and Zn from ingestible ZPRs particles (<250 µm) in 1 M HC*l* at pH<1 and 0.4 M glycine at pH<2.

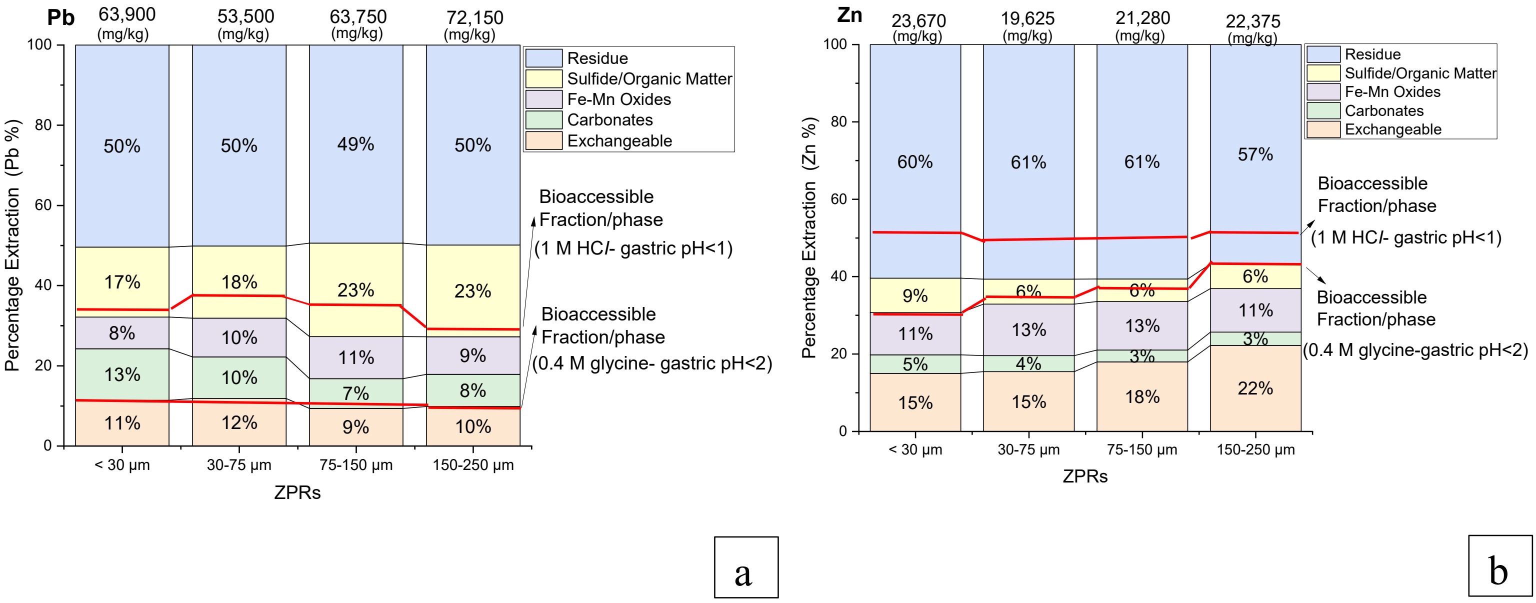


Fig. 6. Cationic speciation of (a) Pb and (b) Zn, with the mean total contents (mg/kg) in (<30 µm, 30-75 µm, 75-150 µm, 150-250 µm particles) of ZPRs. The red line represents the bioaccessible fractions/phase in 1 M HC*l* at conditions of pH<1 and 0.4 M glycine at conditions of pH<2.

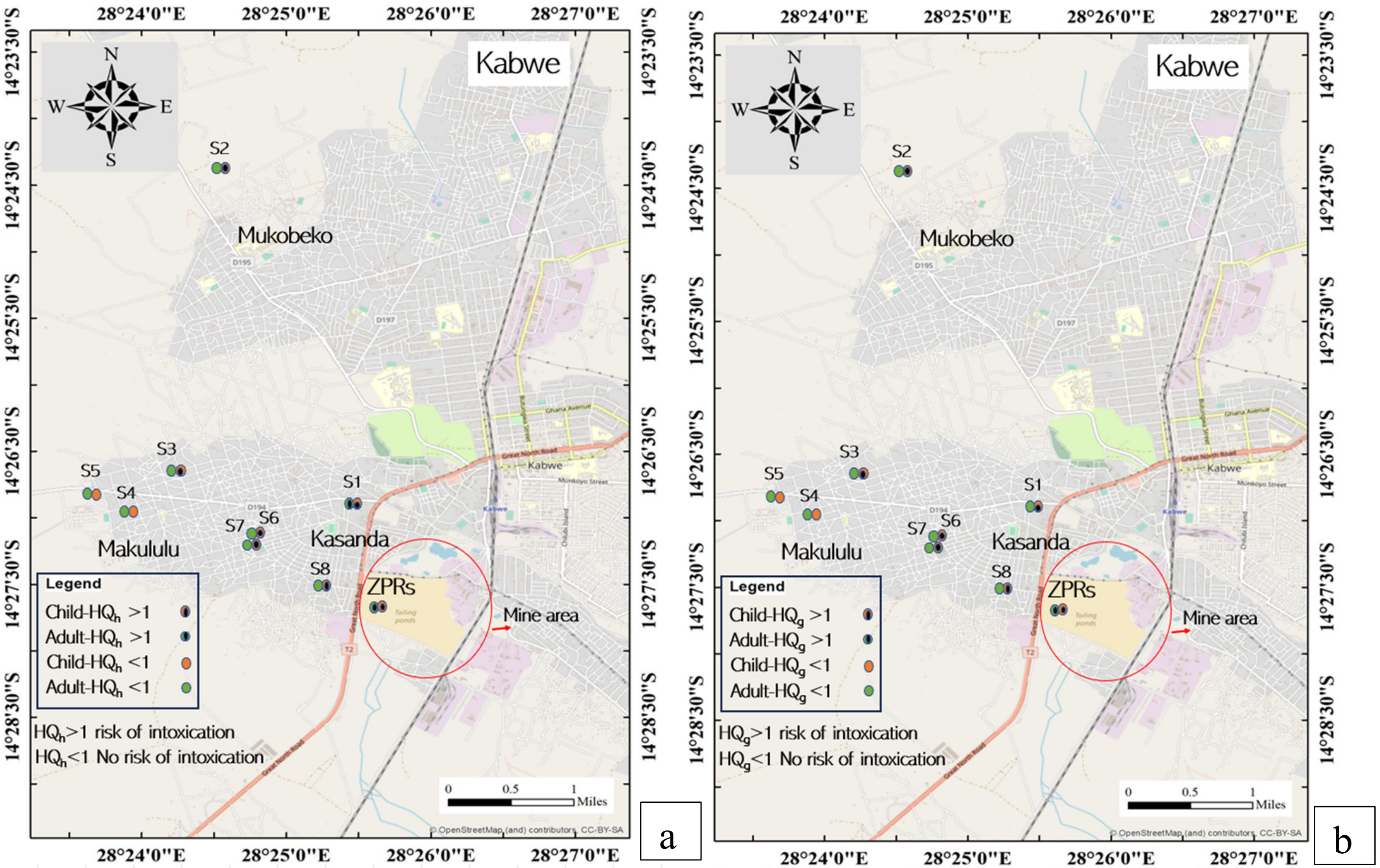


Fig.7. Risk of Pb intoxication for children and adults via Hazard Quotient (*HQ*) in Kabwe, Zambia; (a) $HQ_h$- risks of Pb intoxication through ingestion of ZPRs and soil of (<250 µm) in gastric conditions of pH<1 and (b) $HQ_g$- risks of Pb intoxication through ingestion of ZPRs and soil of (<250 µm) in gastric conditions of pH<2.